Metastin (KiSS-1) Mimetics Identified from Peptide Structure−Activity Relationship-Derived Pharmacophores and Directed Small Molecule Database Screening

Michael J. Orsini,[†] Mark A. Klein,[‡] Mary Pat Beavers,[†] Peter J. Connolly,[†] Steven A. Middleton,[†] and Kevin H. Mayo*[,§]

Department of Biochemistry, Molecular Biology, and Biophysics, University of Minnesota Health Science Center, 6-155 Jackson Hall, 321 Church Street, Minneapolis, Minnesota 55455, Johnson & Johnson Pharmaceutical Research and Development, LLC, 1000 Route 202, Raritan, New Jersey 08869, and Division of Hematology, Oncology, and Transplantation, University of Minnesota, 14-142 PWB, 516 Delaware St. SE, Minneapolis, Minnesota 55455

Received August 14, 2006

Metastin, also known as KiSS-1, the cognate ligand for the metastin receptor GPR54, is a peptide known to dramatically reduce metastasis in experimental models. Despite this, there is no reported structure for metastin nor any small molecule modulators of metastin function that could be used either clinically or experimentally. Here we report the NMR solution structure of a 13-residue metastin peptide in a membrane-like environment (SDS micelles) and find it to have a relatively stable helix conformation from residues 7 to 13. In assays for metastin receptor binding and calcium flux with receptor-transfected HEK-293 cells, we demonstrate through alanine scanning and amino acid substitutions that the peptide C-terminus shows helix periodicity in an NMR structural model and that Phe9, Arg12, and Phe13 are crucial to the activity of the peptide. These three residues lie on one face of the helix and define a pharmacophore site for metastin. We used these pharmacophore features in small molecule database searches to identify hits with submicromolar affinity for the metastin receptor. We also show here that molecules mimicking key elements of this pharmacophore site bind to the metastin receptor and act as full agonists, albeit with reduced potency compared to that of metastin itself. Together this structure−activity approach may yield pharmacologically useful compounds relevant in defining and modulating metastin receptor function.

Introduction

Metastin, also known as kisspeptin or KiSS-1, was first described as a tumor suppressor in 1996.[1,2] Microcell-mediated chromosome transfer was used to identify the gene, first thought to be localized to chromosome 6. Subsequent mapping of KiSS-1 revealed that the gene was actually on chromosome 1,[1,3,4] suggesting that a trans-acting regulator of its expression, perhaps a transcriptional activator, was present on chromosome 6 that permitted its expression. In 2001, an orphan G protein-coupled receptor, termed hOT7T175, was identified as the KiSS-1 receptor.[5] The same receptor was isolated by three different groups and alternately called AXOR12[6] or GPR54.[7] Simultaneously, the ligand, metastin, was identified as a C-terminal amidated peptide of 54, 13, or 10 amino acids in length. The small fragments were the result of metastin proteolysis and were detectable in placental extract as well as in human serum.[5−8] A minimal length of 10 amino acids [YNWNSFGLRF] and C-terminal amidation were found to be critical for biological activity. Transfection of the receptor into highly metastatic melanoma cells followed by administration of KiSS-1 ligand dramatically reduced the number of lung metastases with little or no effect on the primary tumor.[1,3,5]

In the clinic, several analyses suggest that either a reduction in metastin ligand or a reduction in receptor expression correlates with a poorer prognosis and more aggressive metastasis in cancer patients. In esophageal,[9] bladder,[10] gastric,[11] and thyroid cancer[12] patients whose tumors showed a loss of KiSS-1 ligand expression invariably suffered a poorer prognosis and had a greater metastatic potential. In studies of esophageal carcinoma patients, the loss of metastin receptor expression was also observed,[9] while in thyroid cancer, the expression of KiSS-1 and metastin receptor was increased in less aggressive papillary cancers but was decreased in more aggressive follicular adenomas.[12]

The basic biology of metastin and metastin receptor, or what signals and pathways are responsible for its biological action, remains poorly defined. It has been reported that the receptor is exclusively coupled to Gq, activates ERK, and promotes FAK and paxillin phosphorylation and cytoskeletal rearrangement.[5−7] Earlier reports suggest the metastin peptide is a substrate for matrix metalloproteinases and downregulates their expression via the NF-κB pathway.[13,14] A more recent report suggests that the receptor activates a pathway different from other Gq-coupled GPCRs and may upregulate proapoptotic genes that lead to cell cycle arrest and apoptosis.[15] There has also been a recent surge of interest in metastin centered on the regulation of gonadotrophin releasing hormone and its apparently critical role in sexual maturation and control of the hypothalamic−pituitary−gonadal axis.[16,17]

Considering this body of knowledge, it is surprising that little is known about the detailed mechanism through which metastin exerts its biological effects. Furthermore, there appears to be little effort directed toward finding biological or small molecule modulators of metastin, even though there is evidence that the peptide and its receptor might be pharmaceutically attractive targets for intervention against cancer and in the area of reproduction. One reason for this may be the perceived intractability of modulating a peptide receptor with a small molecule therapeutic, combined with the prospect of lengthy and difficult clinical trials to prove benefit from a therapeutic agent targeting metastasis (for reviews on the prospect of tumor suppressors as therapeutics see refs 18 and 19). Nevertheless, approaches exist that allow the design of small molecules based

* To whom correspondence should be addressed. Tel.: 612-625-9968. Fax: 612-624-5121. E-mail: mayox001@umn.edu.
[†] Johnson & Johnson Pharmaceutical Research and Development, LLC.
[‡] University of Minnesota.
[§] University of Minnesota Health Science Center.

10.1021/jm0609824 CCC: $37.00
Published on Web 01/17/2007

on peptide SAR (structure−activity relationship) information. Recently, for example, we reported the ORL-1 (OP4) receptor binding pharmacophore site of the nociceptin peptide 17mer, based on SAR information derived from the NMR[a] (nuclear magnetic resonance spectroscopy) structure and receptor binding and functional assays. Using this SAR approach led to a much higher hit rate than conventional random screening to identify small molecules that interact with the receptor.[20] In this report, we used the same approach to identify a metastin pharmacophore that was useful in database mining of small molecules. These molecules bind the metastin receptor and provide potential leads for further investigation.

Experimental Section

Peptides and Reagents. Metastin was purchased from Phoenix Pharmaceuticals (Belmont, CA) or synthesized by SynPep Corporation. All amino acid substituted peptides of metastin were synthesized by SynPep. ^{125}I-metastin was purchased from Perkin-Elmer Life Sciences. Benzethonium chloride, neuropeptide Y, neuropeptide FF, prolactin releasing peptide **1 (**BIBP 3226) and **2** (GR 231118) were purchased from Sigma.

NMR Measurements. For NMR measurements, freeze-dried peptide was dissolved to 1 mM in water (H_2O or D_2O) or in 100 mM SDS (sodium dodecyl sulfate)/water, and the solution pH was adjusted to pH 5.5 by adding μL quantities of NaOH or HCl to the sample. NMR spectra were acquired at various temperatures between 5 °C and 40 °C on a Varian UNITY Plus-600 NMR spectrometer.

Two-dimensional (2D) homonuclear magnetization transfer (HOHAHA) spectra, obtained by spin-locking with a MLEV-17 sequence[21] with a mixing time of 60 ms, were used to identify spin systems. NOESY (nuclear Overhauser effect spectroscopy) experiments[22] were performed for conformational analysis. All 2D-NMR spectra were acquired in the states-TPPI phase sensitive mode.[23,24] The water resonance was suppressed by direct irradiation (0.8 s) at the water frequency during the relaxation delay between scans as well as during the mixing time in NOESY experiments. 2D-NMR spectra were collected as 512 t1 experiments, each with 2048 complex data points over a spectral width of 8 kHz in both dimensions with the carrier placed on the water resonance. For HOHAHA and NOESY spectra, 8 and 16 scans, respectively, were time averaged per t1 experiment. Data were processed via NMRPipe[25] on an SGI workstation. Data sets were multiplied in both dimensions by a 30 to 60 degree shifted sine-bell function and a Gaussian function. In addition, data sets were also zero-filled in the t1 dimension with linear prediction applied prior to Fourier transformation. To reduce residual solvent noise, residual water was muted on NMRPipe processing.[25]

Backbone NH exchange experiments were performed on metastin peptides in 100 mM SDS/water at pH 5.5. Fresh peptides or hydrogen-exchanged peptides were quickly dissolved in solution immediately prior to acquisition of a series of HOHAHA spectra. Data were processed as described above, and resonance intensities were used to assess relative backbone NH exchange rates. In addition, HOHAHA data were acquired on metastin peptides dissolved in 100 mM SDS/water, as a function of solution temperature, and temperature factors were determined as described in the literature.[26] The presence of relatively low NH temperature factors were taken to indicate involvement of a particular backbone NH in a hydrogen bond.

Structural Modeling. Interproton distance constraints were derived from NOEs (nuclear Overhauser effect) assigned in ^{1}H NOESY spectra acquired with mixing times of 200 and 400 ms. NOEs were classified as strong, medium, weak, very weak, or very, very weak, corresponding to upper bound distance constraints of 2.9, 3.3−3.5, 4.0, 5.0, and 6.0 Å, respectively. The lower bound restraint between nonbonded protons was set to 1.8 Å. Hydrogen bond constraints were identified from the pattern of sequential NOEs involving NH and C_αH protons, initial structure calculations performed without hydrogen bond constraints, and evidence of relatively slow amide proton−solvent exchange and NH temperature factors. Each hydrogen bond identified was defined using two distance constraints: $r_{NH-O} = 1.8$ to 2.5 Å and $r_{N-O} = 2.5$ to 3.3 Å. Final structure calcluations were performed with hydrogen bond restraints.

Derived internuclear distance constraints were used in calculating structures for the metastin peptide by using X-PLOR.[27] Metastin was created using parallhdg.pro force fields. A template coordinate set was generated by using the *Template* routine. The ab initio simulated annealing (SA) protocol was then used. The SA procedure ran high-temperature dynamics (3000 K for 120 ps) and then cooled down to 100 K in 50 K steps with 1.5 ps molecular dynamics at each step. Powell minimization was performed at 100 K for 1000 steps. Structure refinement was done based on simulated annealing starting at 1000 K and ending at 100 K. Final structures were subjected to the X-PLOR Accept routine with the violation threshold for NOEs of 0.5 Å and dihedral angles of 5°. If the Accept routine yielded no or few structures due to restraint violations, various internuclear restraints were either relaxed or removed. In no circumstance were critical backbone interaction restraints removed. Angles, bond lengths, or impropers were not allowed to deviate from ideal geometry more than 5°, 0.05 Å, and 5°, respectively. Structures were superimposed using the viewing program MOLMOL.[28]

Metastin Binding Assay. Binding assays were performed using metastin-expressing membranes purchased from Perkin-Elmer Life Sciences according to manufacturer's directions. Briefly, between 1 and 2 μg of membrane (depending on lot) was added in a 96-well microplate in a total volume of 50 μL binding buffer (50 mM Tris-HCl, pH 7.4, 10 mM $MgCl_2$, 1 mM EDTA). To this was added 1 μL of peptide or compound and 50 μL of ^{125}I-metastin (final concentration, 0.5 nM) diluted in binding buffer supplemented with 0.5% BSA. Binding reactions were incubated at room temperature for 1 h with shaking, then filtered over GF/C filterplates (Perkin-Elmer) prewetted with 0.03% polyethyleneimine. Filters were washed six times with 50 mM Tris-HCl, pH 7.4, and dried under vacuum. Microscint (Perkin-Elmer) in the amount of 30 μL was added per well, and the plates were sealed and counted in a TopCount (Perkin-Elmer). Competition binding curves and K_i values were calculated using GraphPad Prism v.3.0 software.

Metastin Functional Assay. The metastin receptor cloned into the pcDNA3 vector was used to transfect HEK-293 cells, which were then selected using G418. Initial clones were screened using FLIPR-384 (Molecular Devices) to obtain a clone with a high signal/noise ratio and an EC_{50} similar to that reported elsewhere.[6,7] The clone selected had an EC_{50} of 17.3 nM in the calcium flux assay described below and a $K_i = 1.3$ nM, as determined by the previously described metastin receptor binding assay. This cell line was designated 4B1 and used for all experiments. Functional assays were performed by first seeding 96-well black/clear microplates (BD Biosciences) with 80 000 cells/well two days prior to assay. The day of assay, 50 μL of calcium 3 dye (Molecular Devices) was added to the existing 50 μL of media without removal or washing. Cells were incubated for 1 h before initiating experiments. For the assay, 10 1-second baseline images were obtained in the FLIPR-384, and then 25 μL of peptide diluted in water to 5-fold the indicated final concentration was added. Images were then taken once every second for 60 s and then once every 3 s for an additional 60 s. The difference between the peak and baseline fluorescence values was calculated and EC_{50} values were generated using GraphPad Prism v.3.0.

Three-Dimensional Database Searching. Three-dimensional (3D) flex searches were performed using the Unity 4.2 program (Tripos, Inc., 1699 South Hanley Road, St. Louis, Missouri 63144) with implementation of the directed tweak algorithm for conformational searching of the corporate database. Three point queries

[a] Abbreviations: NMR, nuclear magnetic resonance spectroscopy; NOESY, nuclear Overhauser effect spectroscopy; NOE, nuclear Overhauser effect; HTS, high-throughput screening; SDS, sodium dodecyl sulfate; Bztc, benzethonium hydrochloride.

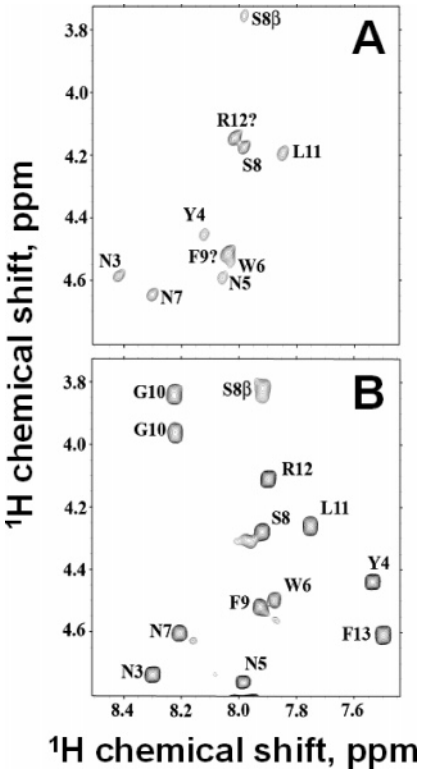

Figure 1. TOCSY spectra for metastin-13 in water and in the presence of SDS. The αN fingerprint regions from 600 MHz ^{1}H NMR TOCSY spectra are shown for metastin in water (A) and in the presence of SDS micelles (B). Peptide concentration was 1 mM in 90% H_2O/10% D_2O, ±100 mM SDS, pH 5.5 and 20 °C. Spectra were accumulated with 2048 k data points over a sweep width of 8000 Hz.

were defined for explicit atom types within the peptide pharmacophore using distance constraints with tolerances of ±1−2 Å. Standard settings were used for the flexible searching. The Unity database was created from the command line starting from a Concord-generated 3D sd file.

Results

NMR Conformational Analysis. Initially we ran NMR spectra for metastin-46, metastin-10, and metsatin-13 in water and in the presence of SDS micelles. Because metastin-46 displayed significant resonance overlap and metastin-10 peptide gave relatively poor NMR spectra, we focused our efforts on metastin-13, which gave acceptable spectra when in solution with SDS micelles. In water, TOCSY αN cross-peaks for metastin-13 are weak and rather broad and not even apparent for some resonance cross-peaks (Figure 1A). In the presence of SDS micelles, metastin-13 displays more well-defined and better dispersed TOCSY αN cross-peaks (Figure 1B). This sample was then used to acquire NOESY data for structure elucidation. Figure 2A (bottom) summarizes backbone to backbone NOEs, along with NH temperature factors and slow NH exchange, observed for metastin-13. The pattern of NOEs suggests formation of helix[29] at the C-terminus from Asn7 to Phe13 and a somewhat less-ordered structure at the N-terminus. Slow exchange of NHs for metastin-13 residues F9, L11, R12, and F13 and $\Delta\delta/\Delta T$ values more positive than −4.5 ppb/K for all residues except L1, P2, N3, G10, and L11 are consistent with the presence of helix. Two variant peptides of metastin-13 (to be discussed further below) were also structurally investigated (bottom of Figure 2B and C), one with an alanine addition (13-i10A11) making a peptide 14mer and one with a G10 deletion (delGly10) making a peptide 12mer.

Conformational modeling was performed using NOE data acquired for metastin-13, 13-i10A11, and delGly10 in the presence of SDS micelles. A total of 294, 300, and 231 NOE distance constraints were derived from analysis of NOESY spectra for each of the peptides, respectively. These include 173, 159, and 125 intraresidue constraints; 95, 69, and 64 sequential constraints; and 26, 72, and 42 medium-range ($|i - j| < 5$) constraints for metastin-13, 13-i10A11, and delGly10, respectively. A total of four hydrogen bonds for metastin-13 could be identified by inspection of long-lived backbone NHs (residues 9, 11, 12, and 13) for metastin-13, in addition to eight hydrogen bonds identified by temperature factors (residues 4−9, 11−13). The combination of these two experiments gave a net of 8 hydrogen bonds and 16 hydrogen bond constraints. No hydrogen bonds could be identified for 13-i10A11 via inspection of long-lived backbone NHs via exchange experiments; however, seven hydrogen bonds could be identified via inspection of temperature factors (residues 4, 6−10, 13, 14), giving rise to 14 hydrogen bond constraints. A total of seven hydrogen bonds could be identified by inspection of long-lived backbone NHs (residues 4, 6−9, 11, 12) for delGly10 in addition to six hydrogen bonds identified by temperature factors (residues 4, 6−9, 11, 12), giving rise to 14 hydrogen bond distance restraints. The total number of experimentally derived constraints was, therefore, 310, 314, and 244 for metastin-13, 13-i10A11, and delGly10, respectively, giving an average of 24, 22, and 20 constraints per residue for metastin-13, 13-i10A11, and delGly10, respectively.

Initially, 100 structures for each peptide were calculated as described in Experimental Section. From the Accept routine in XPLOR, the 33 lowest energy structures for metsatin-13 were selected and are superimposed (backbone C^α atoms) in Figure 2A. These structures showed no NOE violations greater than 0.5 Å and satisfy experimental constraints quite well. Structural statistics are summarized in Table 1. For these 33 structures, the atomic RMS differences with respect to the mean coordinate positions were 0.56 ± 0.16 Å for backbone N, C^α, and C atoms and 1.50 ± 0.27 Å for all heavy atoms. The best defined region in metastin-13 is at the C-terminus with a helix running from Asn7 to Phe13.

For metastin variant peptide 13-i10A11, the 29 lowest energy structures were selected from the Accept routine in XPLOR. These structures are superimposed (backbone C^α atoms) in Figure 2B and also show no NOE violations greater than 0.5 Å and satisfy experimental constraints quite well. Structural statistics are summarized in Table 1. Analysis of these structures shows a well-formed helix running from residue 6 through residue 14, with a less structurally defined N-terminus. For these 29 structures, the atomic RMS differences with respect to the mean coordinate positions were 0.81 ± 0.3 Å for backbone N, C^α, and C atoms and 1.84 ± 0.39 Å for all heavy atoms.

For metastin variant peptide delGly10, the 18 lowest energy structures were selected from the Accept routine in XPLOR. These structures are superimposed (backbone C^α atoms) in Figure 2C, and show no NOE violations greater than 0.5 Å and satisfy experimental constraints quite well. Structural statistics are also summarized in Table 1. In this case, helix runs from residue 2 through residue 12, and the atomic RMS differences with respect to the mean coordinate positions were 0.32 ± 0.14 Å for backbone N, C^α, and C atoms and 1.10 ± 0.20 Å for all heavy atoms.

Metastin Structure−Activity Relationships. Structure is only one component used to define SAR for a peptide. Biological activity is the other. Because metastin is a Gq-coupled

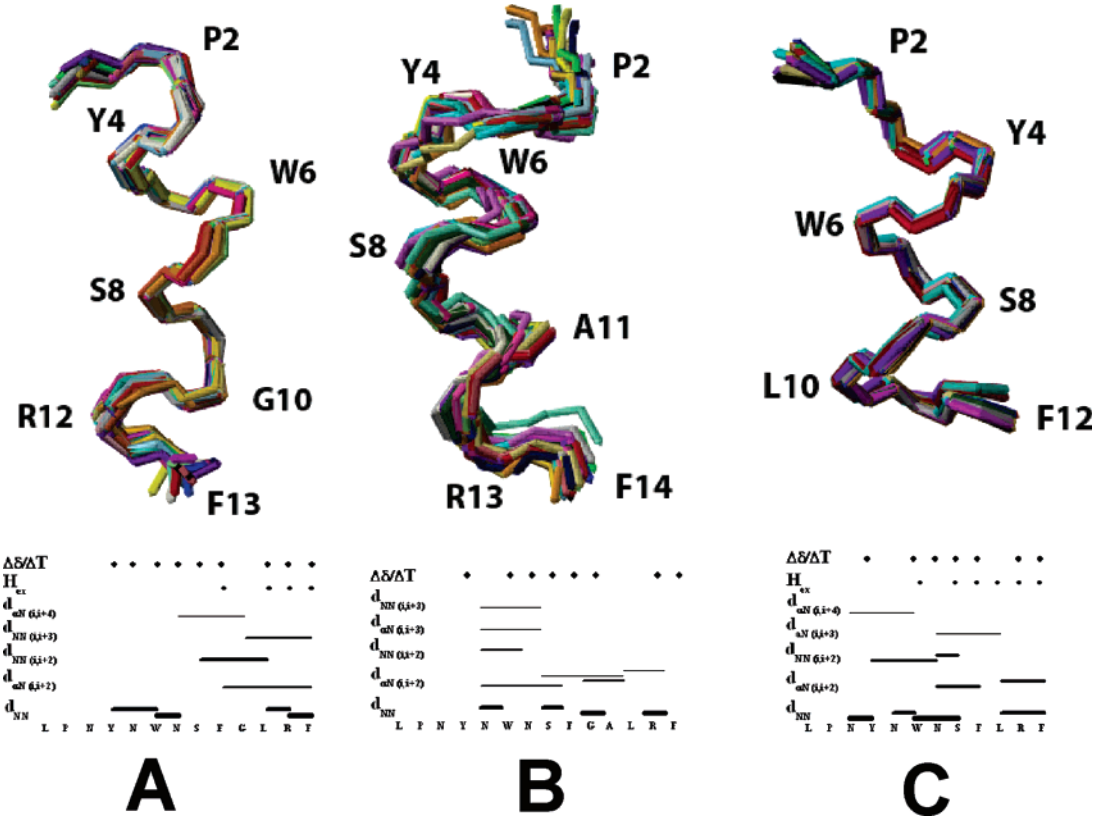

Figure 2. Summary of NOEs and derived structures. Structural information is provided for metastin-13 (A) in SDS, along with two variants: 13-i10A11 (B) and delGly10 (C). Observed backbone-to-backbone NOEs are summarized at the bottom of each set of superimposed structures (Final Accept structures), with the thickness of the bar being proportional to the magnitude of the NOE. Relatively long-lived backbone NHs are indicated by circles and low-temperature factors are indicated with solid squares.

Table 1. Structural Statistics for the Lowest Energy Structures

	13mer[a] (33)	14mer[a] (29)	12mer[a] (18)
	RMS deviations[b] (Å)		
NOE (140)	0.085 ± 0.002	0.084 ± 0.002	0.089 ± 0.004
H-bonds	16	14	14
	deviations from idealized geometry		
bonds (Å)	0.0098 ± 0.0002	0.0096 ± 0.0002	0.0090 ± 0.0003
angles (°)	0.9 ± 0.02	0.97 ± 0.02	1.0 ± 0.02
	energies (kcal·mol^{-1})		
E_{NOE}[c]	110 ± 5	110 ± 5	93 ± 8
E_{bond}	22 ± 0.7	22 ± 1.0	18 ± 1.1
E_{angle}	48 ± 3.5	61 ± 3	57 ± 1.7
E_{total}	200 ± 9	224 ± 8	220 ± 14

[a] The number of structures over which values have been averaged. [b] RMS deviations from experimental distance restraints (Å). None of the final structures exhibited distance restraint violations greater than 0.5 Å or dihedral angle violations greater than 5°. RMSD values represent the mean and standard deviations for the structures. [c] The final values of the NOE (ENOE), torsion angle (ECDIH), and NCS (ENCS) potentials have been calculated with force constants of 50 kcal·mol^{-1}·Å^{-2}, 200 kcal·mol^{-1}·rad^{-2}, and 300 kcal·mol^{-1}·Å $^{-2}$, respectively.

Table 2. Binding of Metastin and Metastin-Derived Peptides to the Metastin Receptor (K_i) and Calcium Release Functional Activity (EC_{50}) of Peptides

peptide	K_i (nM)	EC_{50} (nM)
10-mer[a]	1.3 ± 0.6	17.3 ± 10.7
Y4A	10.5 ± 3.3	33.0 ± 14.8
N5A	21.1 ± 4.7	30.3 ± 14.9
W6A	1.8 ± 0.4	11.3 ± 2.9
N7A	33.4 ± 9.5	39.5 ± 6.6
S8A	0.8 ± 0.3	29.4 ± 15.7
F9A	198.3 ± 38.1	285.0 ± 76.4
G10A	5.0 ± 1.4	22.2 ± 10.4
L11A	29.5 ± 7.7	108.3 ± 38.0
R12A	82.7 ± 11.0	87.8 ± 3.3
F13A	240.2 ± 57.4	347.5 ± 111.4
13-mer	1.1 ± 0.4	22.8 ± 10.9
46-mer	3.1 ± 1.2	30.3 ± 10.4

[a] Results are averaged from a minimum of four experiments performed in duplicate (receptor binding) or triplicate (calcium release).

receptor, we used calcium release as a functional assay together with a competitive metastin receptor binding assay to assess activity on metastin and a number of amino acid substituted variants of metastin-13.

Initially, we performed these assays on metastin-46, metastin-13, and metastin-10 [YNWNSFGLRF]. K_i values (receptor binding) and EC_{50} values (calcium mobilization) are presented in Table 2. The activity of the three peptides in both binding and functional assays were essentially the same; therefore, further substitution studies were performed only on metastin-10. Because the NMR structure was done on metastin-13, we shall hereafter in this section refer to the residues according to the sequential numbering of the 13-mer, that is, Tyr4 through Phe13.

Initially, we performed an alanine scan on metastin-10 and assayed these peptides for receptor binding and calcium release. Representative curves for receptor binding and calcium release are illustrated in Figure 3A and B, respectively. These data are more easily digested by plotting the ratios of receptor binding and calcium release of the variants to those of the parent metastin-10 peptide, as shown in bar graph format in Figure 4A and B. The higher the bar, the more reduced is either receptor binding or signaling relative to that of the native metastin. The correlation coefficient for receptor binding and calcium release is 0.97 ($p < 0.0001$), as shown in Figure 4. From these data, it is apparent that alanine substitutions at Phe9, Arg12, and Phe13

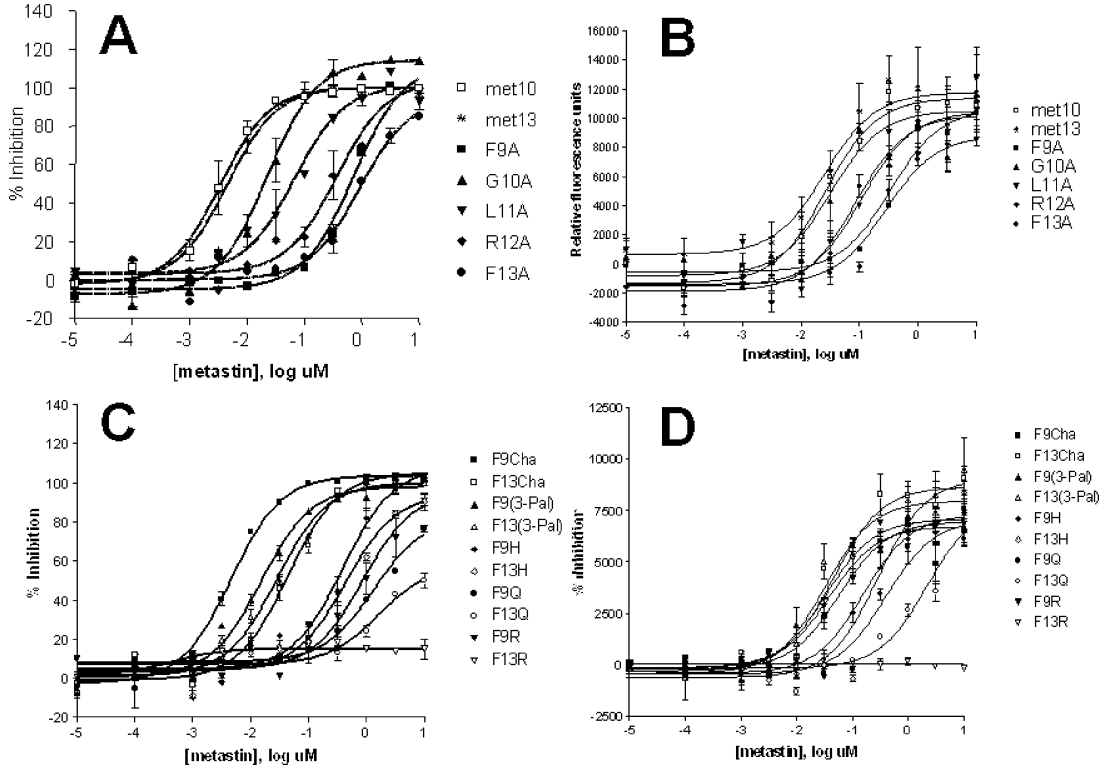

Figure 3. Binding and functional properties of metastin-10 peptide variants. Exemplary dose response curves for competitive metastin receptor binding (A) and calcium release (B) are shown for some alanine substituted variants. Competitive receptor binding and calcium release were performed as described in Experimental Section. Values represent the average of at least four independent experiments. Numerical values for these data are summarized in Table 2.

produce the most dramatic decreases in activity, although another sensitive position is Leu11.

The NMR-derived structure (Figure 2A) indicates that the metastin peptide forms a helix from residue Asn7 to Phe13, which encompasses these functionally key residues. This model has Phe9 and Phe13 lying nearly on top of one another on one face, with Gly10 and Leu11 on the other face, and Arg12 positioned at the side (Figures 2A and 5A). While one cannot conclude definitively from the NMR-derived structure that a helix is the bioactive conformation, further analysis of the alanine scanning data for metastin receptor binding and signaling strongly supports this view. Namely, helix periodicity from Phe9 to Phe13 is reflected in the alanine-substitution activity profiles (Figure 4), where activity is decreased in Phe9Ala (residue *i*) and then again in Arg12Ala ($i + 3$) and more so in Phe13Ala ($i + 4$). Albeit only over one turn of a helix, this is consistent with the NMR-derived structure. In effect, these structure−function relationships yielded a working model for a pharmacophore site of the metastin peptide. This model has the phenyl ring of Phe9 on top of that of Phe13 and flanked by Arg12 and suggests that the metastin peptide, when folded in this fashion, interacts with its receptor via both hydrophobic aromatic ring residues and a positively charged arginine residue. This model can be used to identify novel nonpeptide modulators of metastin receptor as potential drug candidates, as discussed further below.

Chemical Substitutions at the Pharmacophore Site. Having identified a pharmacophore site for metastin, we then needed to determine its sensitivity to chemical substitution. This information is crucial to screen small molecule libraries using search algorithms that rely on selecting spatially related points in a structure and assigning chemical substituents for pharmacophore queries. To this end, we performed an additional round of substitutions limited to residues within the pharmacophore site [Phe9 to Phe13] and screened these variant peptides in the metastin receptor binding and calcium release assays. Results are provided in Table 3.

First, we modified the C-terminal amide to the free acid, which led to a dramatic loss of activity in agreement with previous studies (Table 3).[5] Then, we made a series of substitutions. Substitutions of Phe9 and Phe13 with Tyr, Trp, cyclohexylalanine (CHA), and 3-pyridinylalanine (3-Pal) were well tolerated at both positions, with little or no significant change in either binding affinity or agonist potency. These data indicate that neither position requires an aromatic ring and that both positions tolerate a nitrogen-substituted aromatic ring. Further, a hydrophobic group may be sufficient for activity as reflected by the activity of the cyclohexylalanine substitutions. In contrast, substitution of Phe9 or Phe13 with His, Arg, Leu, or Gln produced significant decreases in both receptor binding affinity and agonist activity. In each case, the effect of substitution at Phe13 was correspondingly greater than that at Phe9, suggesting that Phe9 better tolerates these substitutions. When either Ala or Arg was substituted at Phe9 and Phe13, simultaneously, receptor binding and function were completely lost. Together, these data suggest that positions 9 and 13 prefer a six-membered ring but that aromaticity and nitrogen substitution, as well as distance of the ring from the peptide backbone, are not critical.

Next, we investigated the effect of substitutions at Gly10, Leu11, and Arg12. Based on the helical conformation of the peptide, helix-breaking Pro residues were introduced at Gly10 and Leu11 in two single-substituted variants. Both of these peptides displayed greatly reduced affinity and agonist activity (Table 3) compared to the native peptide. Substitution of Gly10 with Leu also significantly reduced both affinity and activity. At Leu11, substitution with Ile was less tolerated than with Nle. This may be explained, at least in part, by the propensity of Ile to form β structure compared to that of Leu, which has more

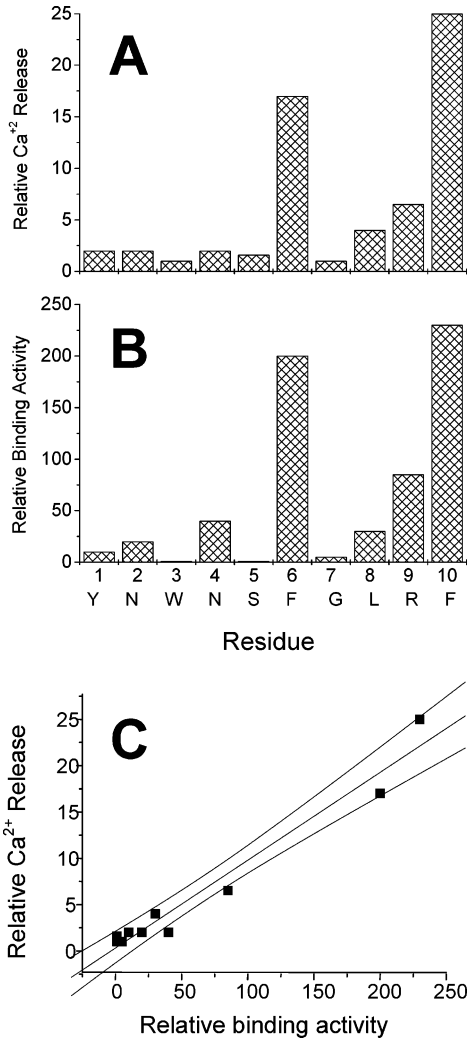

Figure 4. Relative K_i values and functional EC_{50} values for the metastin-10 alanine-scanning substitutions. Data shown in panels A and B were obtained by calculating the natural logarithm of the experimental value for an alanine-substituted peptide divided by the value for native metastin-10. A correlation plot for metastin receptor binding and calcium release is shown as an insert; a standard linear fit gives a correlation coefficient of 0.97.

α-helical potential, and Nle, which has an intermediate propensity.[30] Substitution of Arg12 with Lys was better tolerated than that with Ala, in respect to binding affinity, but only marginally improved in agonist activity (Table 3). In contrast, substitution of Arg12 with citrulline (urea) produced a peptide with Ala-like receptor binding affinity but considerably poorer agonist function. This observation suggests that a positive charge is more important than hydrogen-bonding potential for receptor binding affinity, but less critical for agonist function. In contrast, substitution of Arg12 with β-phenylalanine completely abrogated receptor binding and functional activity. It is likely that the introduction of this bulky hydrophobic group significantly alters interaction with the receptor binding pocket.

To test how much variance may be allowed within the pharmacophore site, we increased and decreased the length of metastin-13 by one residue. Two variants were made: deletion of Gly10 (delGly10) and insertion of an alanine residue between residues Gly10 and Leu11 (13-i10A11). DelGly10 produced an essentially inactive peptide and the alanine insertion variant (13-i10A11) significantly reduced both receptor binding and agonist activity but did not abolish it. To further explore this structure−activity effect, we acquired NMR structural data (described above) on both variants and calculated their NOE-based structures, as was done with parent metastin-13. Backbone superpositions of their calculated structures are illustrated in Figure 2B and C. As can be seen, both variant peptides maintain helical conformation like metastin-13. However, Phe9 and Phe13 in either variant have a different spatial relationship compared to these residues in parent metastin-13. Together these data indicate that the precise spatial arrangement of residues within this pharmacophore site of metastin-13 is crucial to activity.

Table 3. Binding of Metastin-10 Variant Peptides to Metastin Receptor (K_i) and Calcium Release Functional Activity (EC_{50})

peptide	K_i (nM)	EC_{50} (nM)
F9W[a]	7.7 ± 0.8	25.0 ± 9.5
F9Y	16.2 ± 1.6	70.8 ± 30.4
F9L	141.8 ± 27.2	290.3 ± 85.5
F9Cha	2.0 ± 0.6	17.6 ± 8.3
F9H	109.6 ± 28.8	101.4 ± 12.2
F9−3-Pal	4.7 ± 0.7	11.8 ± 4.3
F9Q	298.2 ± 27.4	215.2 ± 65.8
F9R	196.7 ± 49.3	86.7 ± 23.9
F13W	1.6 ± 0.4	33.8 ± 14.4
F13Y	2.2 ± 0.1	46.3 ± 11.3
F13L	80.8 ± 7.2	392.8 ± 107.4
F13Cha	11.1 ± 1.9	91.7 ± 20.0
F13H	161.8 ± 25.4	385.2 ± 71.8
F13-3-Pal	9.3 ± 1.0	102.9 ± 36.5
F13Q	494.9 ± 63.3	2097.3 ± 305.8
F13R	10 000	10 000
F9AF13A	10 000	10 000
F9RF13R	10 000	10 000
delG10	10 000	10 000
G10L	775.2 ± 108.4	791.8 ± 144.8
G10P	10 000	10 000
L11I	51.5 ± 10.9	110.0 ± 29.2
L11Nle	15.8 ± 4.3	25.8 ± 15.6
L11P	10 000	644.8 129.6
R12K	9.4 ± 6.0	69.8 ± 12.5
R12Cit	88.1 ± 7.9	213.7 ± 84.3
R12Bphe	10 000	10 000
13-i10A1	94.8 ± 16.4	290.2 ± 46.3
13(-acid)	551.8 ± 54.0	1068.5 ± 116.1

[a] Results are averaged from a minimum of four experiments performed in duplicate (receptor binding) or triplicate (calcium release).

Small Molecule Database Searching Using the Pharmacophore Model. The metastin peptide SAR highlights the biological relevance of four amino acid side chains, Phe-9, Phe-13, Leu-11, and Arg-12, along with the C-terminal amide group. Three four-point pharmacophore-based search queries were designed that included these biologically relevant chemical features. The first query comprised two phenyl rings representing Phe-9 and Phe-13 phenyl groups, an ionizable basic group representing the positively charged guanidine group of Arg-12, and an isopropyl group to represent the side chain of Leu-11 (Figure 5B). These groups were chosen for the following reasons. Both Phe-9 and Phe-13 substitutions with Tyr residues showed little effect on activity, with these mutants being almost equipotent to the native peptide. Therefore, the phenyl group was used as a feature at both C-terminal Phe locations. Substitution of Arg-12 with a citrulline side chain led to a substantial loss in activity, demonstrating the importance of the positively charged terminus. This was further supported by biological data showing the tolerance of a Lys substitution at Arg-12. From these data, we selected the positively charged terminus as an additional pharmacophore feature. Finally, when Leu-11 was changed to Ala or even Ile, a substantial loss in activity resulted. Therefore, the explicit Leu side chain isopropyl group was specified in the pharmacophore.

The second four-point pharmacophore-based search query was nearly identical to the first, except for the change of the Phe-9

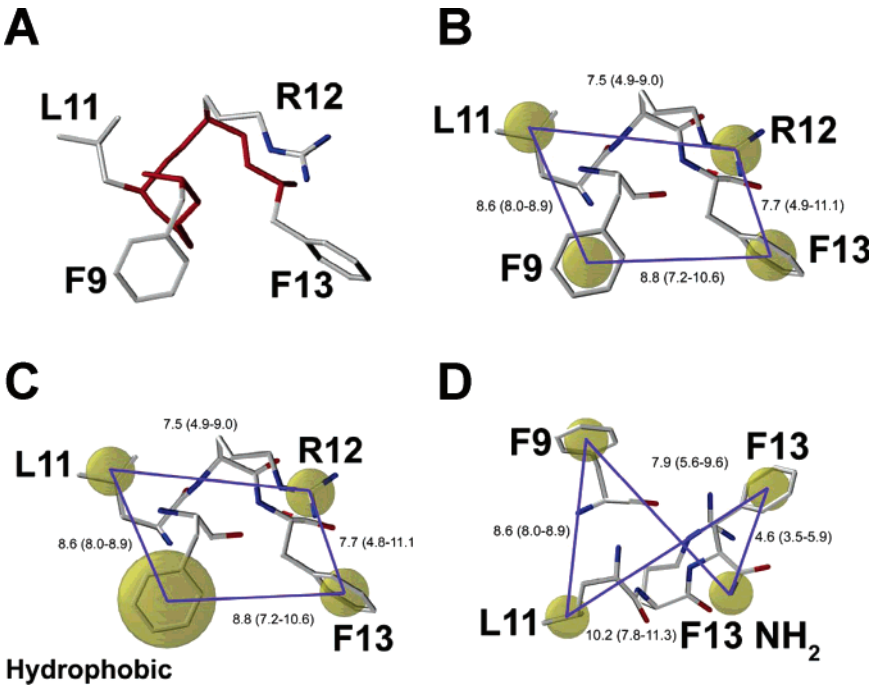

Figure 5. Pharmacophore queries 1, 2, and 3 are shown superimposed over the lowest energy NMR-derived structure of metastin-13. (A) The lowest energy NMR-derived structure of metastin-13 exhibiting residues F9 through F13 is shown with the backbone atoms in red, side chain atoms in gray, and guanidinium nitrogens in blue. (B) Distance constraints for F9, L11, R12, and F13 with side chain centroids represented as spheres are shown superimposed with blue lines representing distance constraints. Also labeled are the mean distance constraints between pharmacophore points with the highest and lowest distances for each constraint from the 33 lowest energy NMR-derived structures from metastin-13. (C) Same as for (B), with the exception of a general hydrophobic constraint replacing the centroid for F9. (D) Distance constraints for F9, L11, F13, and F13 C-terminus amide with side chain centroids represented as spheres shown superimposed with blue lines representing distance constraints. Distances are as for B and C.

Table 4. Screening Data for Metastin Pharmacophores

number[a]	pharmacophore features[a]	hit rate[a] (for 50% inhibition)	hit rate[a] (for 60% inhibition)
1	2 phenyl, positive ionizable, isopropyl	61/836 = 7.3%	50/836 = 6.0%
2	2 hydrophobic, positive ionizable, isopropyl	86/595 = 14.4%	50/595 = 8.4%
3	2 hydrophobic, isopropyl, amide	24/366 = 6.6%	19/366 = 5.2%

[a] The number of the pharmacophore refers to the description in the text, the features of each pharmacophore are noted, and the hit rate is based on percent inhibition of ^{125}I-metastin-10 in a competitive receptor binding assay performed at a screening concentration of 10 μM. The number of hits and hit rates are provided for a cutoff of either 50% or 60% inhibition.

phenyl feature to a general hydrophobic group (Figure 5C). This change in the query was made because the peptide SAR demonstrated that the Phe-9-CHA substitution had no significant effect on activity (Table 3), illustrating the importance of a large bulky hydrophobic group, but not necessarily an aromatic group, at that position.

The third four-point query used the Leu-11 isopropyl group, the Phe-9 hydrophobic group, and the Phe-13 phenyl group, together with the C-terminal amide (Figure 5D). The C-terminal amide was included in this query because deamidation to the free acid form was shown to significantly inhibit both receptor binding and agonist function (Table 3).

To demonstrate that these pharmacophore-based queries could lead to small molecule hits that possessed affinity for the metastin receptor, the corporate Johnson & Johnson library was searched using these three pharamacophore queries, which resulted in identification of nearly 2000 compounds. These compounds were assayed using competitive receptor binding at a concentration of 10 μM for the initial screen. Screening data are summarized in Table 4. Hit rates range from 5.2% to 8.4% using 60% inhibition of binding at a 10 μM screening concentration as the cutoff. Relaxing the cutoff to 50% inhibiton of binding did not yield an appreciable increase in hits, with the exception of the second pharmacophore, which imposed the broader condition of hydrophobicity rather than an explicit phenyl group at the Phe-9 and Phe-13 positions. These hit rates exceed the expected 0.5% to 1% hit rate typically observed with random high-throughput screening (HTS).

To further explore the quality of these compounds, we selected a total of 55 compounds that demonstrated 80% or greater inhibition of metastin binding at the 10 μM screening concentration and obtained K_i values for metastin receptor binding. This represents an overall hit rate of 3.1% (55 compounds of 1797 screened). Of these 55 compounds, 21 (38%, 1.2% of 1797 screened compounds) exhibited K_i values equal to or less than 1 μM, with the most potent compound having a K_i of 0.29 μM.

We then tested these 21 compounds further for functional activity as agonists or antagonists. For agonist activity, compounds were added directly to cells expressing metastin receptor and assayed as described for peptides in Experimental Section. We discovered four compounds with detectable agonist activity compared to vehicle background, ranging from 11 to 38% of maximal activity, which was defined as the maximal calcium mobilization exhibited by 10 μM metastin 10-mer. Two compounds were derived from pharmacophore-based query 1 and one each from pharmacophore-based queries 2 and 3. The compound with the best agonist activity, **3** (JNJ-8706646)[31]

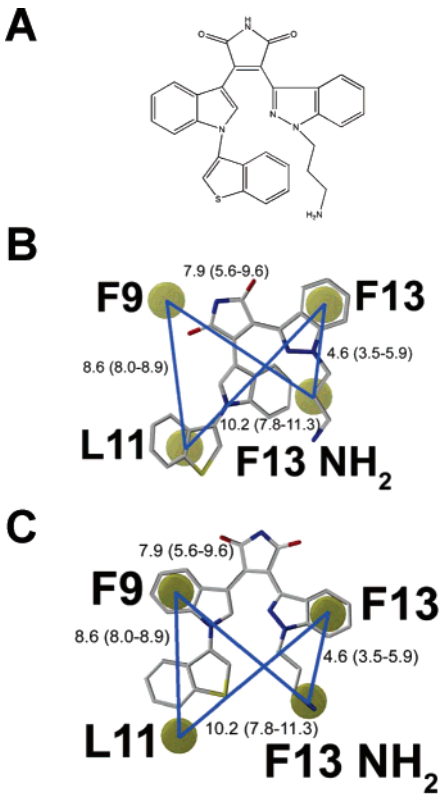

Figure 6. Chemical structure of **3** and the NMR-derived pharmacophore site. (A) The chemical structure of our best agonist, **3**, is shown in 2D. This compound is 38% active (calcium release assay) at 10 μM and has a $K_i = 0.708$ μM for metastin receptor binding. (B) The energy minimized **3** is superimposed over pharmacophore-based query 3. (C) Compound **3** is superimposed over pharmacophore-based query 3 in 3D. The final molecule structure is shown distorted compared to the minimized structure in Figure 6B to show how bond rotation could fit the pharmacophore-based query. Distance constraints for B and C are the same as for that in Figure 5D.

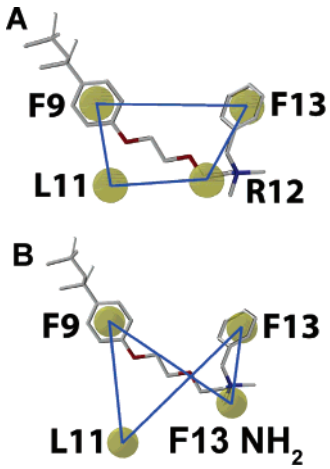

Figure 7. Structures of benzethonium chloride is shown superimposed over pharmacophore-based queries 1 and 3 in A and B, respectively.

(Figures 6 and 7), was identified using pharmacophore-based query 3. This compound displayed a K_i value of 708 nM in the metastin receptor binding assay. Of the remaining compounds that were devoid of detectable agonist activity, none demonstrated the ability to inhibit calcium mobilization elicited by 1 μM metastin peptide 10-mer, even at compound concentrations up to 10 μM. In contrast, the metastin 10-mer and the four compounds with agonist activity demonstrated typical receptor desensitization that was dose-dependent and proportional to their potency as agonists (data not shown).

Given that **3** was the best compound identified from our search, we wanted to compare that structure with the orientation of residues Phe9, Arg12, and Phe13 from the NMR-derived metastin pharmacophore-based query 3. The 2D chemical structure of **3** is shown in Figure 6A, while **3** is shown overlapping pharmacophore-based query 3 in Figure 6B and C. Figure 6B compares pharmacophore-based query 3 with an energy-minimized 3D model of **3**, showing how the query points corresponding to the F13 aromatic, C-terminus amide, and L11 hydrophobic groups correspond to an aromatic group, amine, and hydrophobic group from **3**. Figure 6C shows an alternative structure where the sulfur-containing aromatic group of **3** was allowed to rotate. Here query 3 points corresponding to aromatics from F9 and F13 match aromatics from **3**, and the guanidinium from query 3 corresponds to the amine from **3**.

Furthermore, differences in distances (see the triangles) among these peptide variants parallel differences in the functional data. Peptide delGly10 has inter-residue distances that are closer to those of metastin-13 than of peptide 13-i10A11 and is also more biologically active in the metastin assays than peptide 13-i10A11. Once again, this supports our NMR structure-derived pharmacophore model and provides some limits on allowed structural variance to the model.

Discussion

Here we employed a peptide SAR approach, combining NMR structural studies, receptor binding, and a functional assay, to identify a pharmacophore for metastin. Our initial SAR studies on metastin peptide demonstrate that functionally key amino acid residues are Phe9, Arg12, and Phe13, along with the C-terminal amide group and to a lesser extent Leu11. This information alone indicates that metastin behaves similarly to other members of the RF-amide family of receptors that include prolactin-releasing peptide and neuropeptide FF in which the C-terminal Arg-Phe is critical for activity.[32,33] With metastin, our data show that although positions 9 and 13 prefer a six-membered ring, aromaticity and distance of the ring from the peptide backbone are not crucial. Further, a positively charged nitrogen at the terminus of Arg 12 is not necessary because an amide terminus is also tolerated at this position. A similar though less extensive SAR study done with neuropeptide FF[32] showed that its C-terminal phenylalanine residue appeared to be much less tolerant than that of metastin to substitutions that shortened or lengthened the distance of the aromatic ring from the peptide backbone. However, similar to metastin, substitution of alanine at the C-terminal phenylalanine dramatically reduced the affinity and activity of NPFF. In addition, various studies using invertebrate RW-amide peptides as metastin ligands suggest that tryptophan is well tolerated at the C-terminal position.[34] Thus, access to a hydrophobic pocket on the receptor may be the principal function of these residues.

Lange et al.[35] suggested that molecules that mimic the C-terminal structure of an RF-amide peptide could act as agonists for the RF-family of receptors. For example, benzethonium hydrochloride (Bztc; Figure 7) activates an RF-amide receptor present in locust oviducts.[35] The locust oviduct RF-amide peptide has a C-terminal sequence of Val-Phe-Leu-Arg-Phe, whereas metastin has Phe-Gly-Leu-Arg-Phe. Bztc mimics the structure of metastin in the C-terminal portion of the peptide because it possesses two phenyl rings that resemble the two Phe residues, a positively charged group similar to Arg-H^+ and an isoleucyl group. Because metastin belongs to the RF-amide

family of peptides, we tested whether Bztc could also bind to and activate the metastin receptor. Bztc does indeed bind to the metastin receptor with a rather weak K_i of 3.6 μM, and although Bztc is functionally considerably less potent than metastin, it is nonetheless able to evoke a signal in the calcium release assay of similar magnitude to metastin, albeit at a concentration of 100 μM. Interestingly, a similar compound in our library (JNJ-1148108) that differs from Bztc only by the presence of a methyl group on the first phenyl ring, also binds to and activates metastin receptor with a potency like that of Bztc. Similar to our results, Bztc was less potent on the oviduct receptor than the native ligand.[35] It is possible that information in the N-terminal region of the peptide, as well as C-terminal amidation, which are both absent from Bztc, are required for optimal binding and function. Pharmacophore queries 1 and 3 superimpose well on Bztc (Figure 7). These results appear to validate the main features of our metastin peptide SAR studies. These compounds may provide the basis for further optimization of a small molecule agonist, as well as for other receptor modulators.

Other RF- or RY-amide peptide agonists and antagonists might also display binding or functional activity toward the metastin receptor. Reasoning for this lies in the observation that neuropeptide Y ligands bind to the neuropeptide FF receptor[36,37] and act as antagonists, and prolactin-releasing peptide binds to and activates the neuropeptide FF receptor.[38] However, we found that none of the following compounds, neuropeptide Y, neuropeptide FF, prolactin-releasing peptide (12−31), the mixed NPY1 antagonist/NPY4 agonist **2**, or the NPY1 antagonist **1**, could effectively compete with metastin-10 for binding to the metastin receptor. Only **1**, when tested at concentrations up to 100 μM, displayed a modest ability to displace metastin-10. In addition, none of these peptides or compounds displayed either agonist or antagonist activity toward the metastin receptor in the calcium release assay (data not shown). In contrast, **1** and **2** were reported to displace NPFF binding to their receptor with affinities of between 50 nM and 100 nM,[36] and prolactin releasing peptide was reported to have an EC_{50} of 170 nM on the NPFF receptor.[38] Thus, interaction of metastin with metastin receptor appears to have fundamentally distinct properties compared to other RF-amide family members.

In contrast to our binding assay, Niida et al. have utilized an assay system in yeast in which downsized metastin (45−54) peptide or peptide analog activity was determined via quantification of a β-galactosidase activity encoded by a pheromone-sensitive FUS1-lacZ reporter gene.[39] In alanine-scanning experiments, they also found that substitution of Phe50 and Phe54 (corresponding to Phe9 and Phe13 in our nomenclature) resulted in a complete loss of agonistic activity. Substitution of Leu52 showed complete loss of activity in contrast to our results (decreased but not ablated activity), and substitution of Arg53 yielded a decrease in activity in contrast to our results (ablation of activity). One possible explanation for this discrepancy could be due to differences in the assay technique.

Niida et al. also discovered that amino acid stereochemistry is important, as substitution of N48, Phe50, Gly 51, Leu52, Arg53, and Phe54 with the corresponding D-amino acid (D-Ala in the case of Gly51) significantly decreased peptide agonist activity. Interestingly, cyclized peptides consisting of the five terminal amino acids or various substitutions yielded no agonist activity in the assay, which suggests that the critical pharmacophore site is perturbed from an ideal binding conformation. These findings also support and compliment our results that are consistent with terminal alpha-helical structure being necessary for effective binding.

Aside from identifying functionally key residues in metastin, we have also produced a refined "working model" for a metastin pharmacophore based on a more complete SAR on the metastin peptide. This refined pharmacophore has two six-membered (or greater) aromatic or alkyl (with or without nitrogen substitution) rings (Phe9 and Phe 13 in metastin-13) on top of one another and proximal to a positively charged group (Arg 12 in metastin-13) as well as to an amide moiety (the amidated C-terminus of the metastin peptide). This metastin pharmacophore, and the use of a pharmacophore-based approach to this peptide ligand as opposed to random HTS, is validated by several observations. First, compounds with submicromolar affinity were identified, among which were several weak agonists from the primary screen. Second, benzethonium chloride, which mimics many properties we selected for our pharmacophore, also displays potent binding and agonist activity toward the metastin receptor. Third, random screening is rarely optimal for the more complicated interaction between peptide ligands and their cognate receptors. Random HTS hits are distributed among a wide variety of structural types and likely reflect many different binding modes, whereas a structure-derived pharmacophore search yields compounds that should be similar with regard to the disposition of key functional groups and, therefore, have a higher probability of binding to the corresponding receptor in a manner similar to the native peptide. Because it is likely that a large number of compounds in any small molecule-based library possess aromatic, positive ionizable or leucinyl-like groups, the spatial releationships imparted by a 3D model are critical to explicitly define those compounds in a way that is most likely to mimic the native peptide interaction with receptor. Our results indicate that a pharmacophore-based selection process is advantageous in screening compounds and can significantly reduce the time and effort expended to find lead compounds. This SAR-based pharmacophore approach was also applied successfully in identifying ligands of the nociceptin (ORL-1, OP4) receptor.[20]

Conclusions

Our directed SAR approach with metastin peptide has identified compounds from the corporate library that have measurable agonist activity toward the metastin receptor. Clearly, because compounds identified by the pharmacophore screen failed to approach the affinity and potency of the native ligand, one must consider the N-terminal portion of the metastin peptide as well as the receptor bound-state structure of the ligand to derive small molecules with full agonist properties. In addition, directed analog synthesis will likely be required to endow these molecules with optimized functional properties. Last, our directed SAR approach was shown to be more efficient than random HTS. Given the paucity of structural data available for G protein-coupled receptors, the ability to rapidly identify small molecule leads by other means is of paramount importance.

Acknowledgment. This work was supported by Johnson & Johnson Pharmaceutical Research and Development, LLC. M.A.K. was supported in part by a T-32 Hematology Training Grant from the National Institutes of Health (5T32HL07062). M.J.O. and M.A.K. contributed equally to this work.

References

(1) Lee, J. H.; Miele, M. E.; Hicks, D. J.; Phillips, K. K.; Trent, J. M.; Weissman, B. E.; Welch, D. R. KiSS-1, a novel human malignant melanoma metastasis-suppressor gene. *J. Natl. Cancer Inst.* **1996**, *88*, 1731−1737.

(2) Lee, J. H.; Welch, D. R. Identification of highly expressed genes in metastasis-suppressed chromosome 6/human malignant melanoma hybrid cells using subtractive hybridization and differential display. *Int. J. Cancer* **1997**, *71*, 1035−1044.
(3) Lee, J. H.; Welch, D. R. Suppression of metastasis in human breast carcinoma MDA-MB-435 cells after transfection with the metastasis suppressor gene, KiSS-1. *Cancer Res.* **1997**, *57*, 2384−2387.
(4) West, A.; Vojta, P. J.; Welch, D. R.; Weissman, B. E. Chromosome localization and genomic structure of the KiSS-1 metastasis suppressor gene (KISS1). *Genomics* **1998**, *54*, 145−148.
(5) Ohtaki, T.; Shintani, Y.; Honda, S.; Matsumoto, H.; Hori, A.; Kanehashi, K.; Terao, Y.; Kumano, S.; Takatsu, Y.; Masuda, Y.; Ishibashi, Y.; Watanabe, T.; Asada, M.; Yamada, T.; Suenaga, M.; Kitada, C.; Usuki, S.; Kurokawa, T.; Onda, H.; Nishimura, O.; Fujino, M. Metastasis suppressor gene KiSS-1 encodes peptide ligand of a G-protein-coupled receptor. *Nature* **2001**, *411*, 613−617.
(6) Muir, A. I.; Chamberlain, L.; Elshourbagy, N. A.; Michalovich, D.; Moore, D. J.; Calamari, A.; Szekeres, P. G.; Sarau, H. M.; Chambers, J. K.; Murcock, P.; Steplewski, K.; Shabon, U.; Miller, J. E.; Middleton, S. E.; Darker, J. G.; Larminie, C. G.; Wilson, S.; Bergsma, D. J.; Emson, P.; Faull, R.; Philpott, K. L.; Harrison, D. C. AXOR12, a novel human G protein-coupled receptor, activated by the peptide KiSS-1. *J. Biol. Chem.* **2001**, *276*, 28969−28975 (Epub 22001 May 28931).
(7) Kotani, M.; Detheux, M.; Vandenbogaerde, A.; Communi, D.; Vanderwinden, J. M.; Le Poul, E.; Brezillon, S.; Tyldesley, R.; Suarez-Huertz, N.; Vandeput, F.; Blanpain, C.; Schiffmann, S. N.; Vassart, G.; Parmentier, M. The metastasis suppressor gene KiSS-1 encodes kisspeptins, the natural ligands of the orphan G protein-coupled receptor GPR54. *J. Biol. Chem.* **2001**, *276*, 34631−34636 (Epub 32001 Jul 34616).
(8) Horikoshi, Y.; Matsumoto, H.; Takatsu, Y.; Ohtaki, T.; Kitada, C.; Usuki, S.; Fujino, M. Dramatic elevation of plasma metastin concentrations in human pregnancy: metastin as a novel placenta-derived hormone in humans. *J. Clin. Endocrinol. Metab.* **2003**, *88*, 914−919.
(9) Ikeguchi, M.; Yamaguchi, K.; Kaibara, N. Clinical significance of the loss of KiSS-1 and orphan G-protein-coupled receptor (hOT7T175) gene expression in esophageal squamous cell carcinoma. *Clin. Cancer Res.* **2004**, *10*, 1379−1383.
(10) Sanchez-Carbayo, M.; Capodieci, P.; Cordon-Cardo, C. Tumor suppressor role of KiSS-1 in bladder cancer: loss of KiSS-1 expression is associated with bladder cancer progression and clinical outcome. *Am. J. Pathol.* **2003**, *162*, 609−617.
(11) Dhar, D. K.; Naora, H.; Kubota, H.; Maruyama, R.; Yoshimura, H.; Tonomoto, Y.; Tachibana, M.; Ono, T.; Otani, H.; Nagasue, N. Downregulation of KiSS-1 expression is responsible for tumor invasion and worse prognosis in gastric carcinoma. *Int. J. Cancer* **2004**, *111*, 868−872.
(12) Ringel, M. D.; Hardy, E.; Bernet, V. J.; Burch, H. B.; Schuppert, F.; Burman, K. D.; Saji, M. Metastin receptor is overexpressed in papillary thyroid cancer and activates MAP kinase in thyroid cancer cells. *J. Clin. Endocrinol. Metab.* **2002**, *87*, 2399.
(13) Takino, T.; Koshikawa, N.; Miyamori, H.; Tanaka, M.; Sasaki, T.; Okada, Y.; Seiki, M.; Sato, H. Cleavage of metastasis suppressor gene product KiSS-1 protein/metastin by matrix metalloproteinases. *Oncogene* **2003**, *22*, 4617−4626.
(14) Yan, C.; Wang, H.; Boyd, D. D. KiSS-1 represses 92-kDa type IV collagenase expression by down-regulating NF-kappa B binding to the promoter as a consequence of Ikappa Balpha-induced block of p65/p50 nuclear translocation. *J. Biol. Chem.* **2001**, *276*, 1164−1172.
(15) Becker, J. A.; Mirjolet, J. F.; Bernard, J.; Burgeon, E.; Simons, M. J.; Vassart, G.; Parmentier, M.; Libert, F. Activation of GPR54 promotes cell cycle arrest and apoptosis of human tumor cells through a specific transcriptional program not shared by other Gq-coupled receptors. *Biochem. Biophys. Res. Commun.* **2005**, *326*, 677−686.
(16) Seminara, S. B.; Messager, S.; Chatzidaki, E. E.; Thresher, R. R.; Acierno, J. S., Jr.; Shagoury, J. K.; bo-Abbas, Y.; Kuohung, W.; Schwinof, K. M.; Hendrick, A. G.; Zahn, D.; Dixon, J.; Kaiser, U. B.; Slaugenhaupt, S. A.; Gusella, J. F.; O'Rahilly, S.; Carlton, M. B.; Crowley, W. F., Jr.; Aparicio, S. A.; Colledge, W. H. The GPR54 gene as a regulator of puberty. *N. Engl. J. Med.* **2003**, *349*, 1614−1627.
(17) Colledge, W. H. GPR54 and puberty. *Trends Endocrinol. Metab.* **2004**, *15*, 448−453.
(18) Steeg, P. S.; Ouatas, T.; Halverson, D.; Palmieri, D.; Salerno, M. Metastasis suppressor genes: basic biology and potential clinical use. *Clin. Breast Cancer* **2003**, *4*, 51−62.
(19) Steeg, P. S. Metastasis suppressors alter the signal transduction of cancer cells. *Nat. Rev. Cancer* **2003**, *3*, 55−63.
(20) Orsini, M. J.; Nesmelova, I.; Young, H. C.; Hargittai, B.; Beavers, M. P.; Liu, J.; Connolly, P. J.; Middleton, S. A.; Mayo, K. H. The nociceptin pharmacophore site for opioid receptor binding derived from the NMR structure and bioactivity relationships. *J. Biol. Chem.* **2005**, *280*, 8134−8142 (Epub 2004 Dec 8113).
(21) Bax, N.; Davis, D. G. MLEV-17-based two-dimensional homonuclear magnetization transfer spectroscopy. *J. Magn. Reson.* **1985**, *65*, 355−360.
(22) Wider, G.; Macura, S.; Kumar, S.; Ernst, R. R.; Wüthrich, K. Homonuclear two-dimensional ^{1}H NMR of proteins. Experimental procedures. *J. Magn. Reson.* **1984**, *56*, 207−234.
(23) States, D. J.; Haberkorn, R. A.; Ruben, D. J. A two-dimensional nuclear overhauser experiment with pure absorption phase in four quadrants. *J. Magn. Reson.* **1982**, *48*, 286−292.
(24) Bodenhausen, G.; Vold, R. L.; Vold, R. R. Multiple quantum spin-echo spectroscopy. *J. Magn. Reson.* **1980**, *37*, 93−106.
(25) Delaglio, F.; Grzesiek, S.; Vuister, G. W.; Zhu, G.; Pfeifer, J.; Bax, A. NMRPipe: a multidimensional spectral processing system based on UNIX pipes. *J. Biomol. NMR* **1995**, *6*, 277−293.
(26) Baxter, N. J.; Williamson, M. P. Temperature dependence of ^{1}H chemical shifts in proteins. *J. Biomol. NMR* **1997**, *9*, 359−369.
(27) Brunger, A. T. *X-Plor. A system for X-ray crystallography and NMR*; Yale University Press: New Haven, 1992.
(28) Koradi, R.; Billeter, M.; Wuthrich, K. MOLMOL: a program for display and analysis of macromolecular structures. *J. Mol. Graphics* **1996**, *14*, 29−32, 51−55.
(29) Wuthrich, K. *NMR of Proteins and Nucleic Acids*; Wiley-Interscience: New York, 1986.
(30) Arfmann, H. A.; Labitzke, R.; Wagner, K. G. Conformational properties of L-leucine, L-isoleucine, and L-norleucine side chains in L-lysine copolymers. *Biopolymers* **1977**, *16*, 1815−1826.
(31) Zhang, H.-C.; Maryanoff, B.; Conway, B.; White, K.; Ye, H.; Hecker, L. R.; McComsey, D. F. Preparation of indazolyl-substituted pyrroline compounds as kinase inhibitors for treating or ameliorating kinase-mediated disorders. PCT Int. Appl. 2002, WO 2002046183, 2002.
(32) Mazarguil, H.; Gouarderes, C.; Tafani, J. A.; Marcus, D.; Kotani, M.; Mollereau, C.; Roumy, M.; Zajac, J. M. Structure-activity relationships of neuropeptide FF: role of C-terminal regions. *Peptides* **2001**, *22*, 1471−1478.
(33) Gicquel, S.; Mazarguil, H.; Desprat, C.; Allard, M.; Devillers, J. P.; Simonnet, G.; Zajac, J. M. Structure-activity study of neuropeptide FF: contribution of N-terminal regions to affinity and activity. *J. Med. Chem.* **1994**, *37*, 3477−3481.
(34) Clements, M. K.; McDonald, T. P.; Wang, R.; Xie, G.; O'Dowd, B. F.; George, S. R.; Austin, C. P.; Liu, Q. FMRFamide-related neuropeptides are agonists of the orphan G-protein-coupled receptor GPR54. *Biochem. Biophys. Res. Commun.* **2001**, *284*, 1189−1193.
(35) Lange, A. B.; Orchard, I.; Wang, Z.; Nachman, R. J. A nonpeptide agonist of the invertebrate receptor for SchistoFLRFamide (PDVDH-VFLRFamide), a member of a subfamily of insect FMRFamide-related peptides. *Proc. Natl. Acad. Sci. U.S.A.* **1995**, *92*, 9250−9253.
(36) Mollereau, C.; Gouarderes, C.; Dumont, Y.; Kotani, M.; Detheux, M.; Doods, H.; Parmentier, M.; Quirion, R.; Zajac, J. M. Agonist and antagonist activities on human NPFF(2) receptors of the NPY ligands GR231118 and BIBP3226. *Br. J. Pharmacol.* **2001**, *133*, 1−4.
(37) Mollereau, C.; Mazarguil, H.; Marcus, D.; Quelven, I.; Kotani, M.; Lannoy, V.; Dumont, Y.; Quirion, R.; Detheux, M.; Parmentier, M.; Zajac, J. M. Pharmacological characterization of human NPFF(1) and NPFF(2) receptors expressed in CHO cells by using NPY Y(1) receptor antagonists. *Eur. J. Pharmacol.* **2002**, *451*, 245−256.
(38) Engstrom, M.; Brandt, A.; Wurster, S.; Savola, J. M.; Panula, P. Prolactin releasing peptide has high affinity and efficacy at neuropeptide FF2 receptors. *J. Pharmacol. Exp. Ther.* **2003**, *305*, 825−832 (Epub 2003 Feb 2020).
(39) Niida, A.; Wang, Z.; Tomita, K.; Oishi, S.; Tamamura, H.; Otaka, A.; Navenot, J. M.; Broach, J. R.; Peiper, S. C.; Fujii, N. Design and synthesis of downsized metastin (45−54.) analogs with maintenance of high GPR54 agonistic activity. *Bioorg. Med. Chem. Lett.* **2006**, *16*, 134−137.

JM0609824